

# Lifetimes of high-spin states in $^{74}\text{Kr}$

J.J. Valiente-Dobón<sup>a,b</sup>, C.E. Svensson<sup>a</sup>, T. Steinhardt<sup>c</sup>, A.V. Afanasjev<sup>d,e</sup>,  
I. Ragnarsson<sup>f</sup>, C. Andreoiu<sup>a,g</sup>, R.A.E. Austin<sup>h</sup>, M.P. Carpenter<sup>i</sup>,  
D. Dashdorj<sup>j</sup>, G. de Angelis<sup>b</sup>, F. Dönau<sup>k</sup>, J. Eberth<sup>c</sup>, E. Farnea<sup>l</sup>,  
S.J. Freeman<sup>i</sup>, A. Gadea<sup>b</sup>, P.E. Garrett<sup>a,m</sup>, A. Gørgen<sup>n</sup>, G.F. Grinyer<sup>a</sup>,  
B. Hyland<sup>a</sup>, D. Jenkins<sup>o</sup>, F. Johnston-Theasby<sup>o</sup>, P. Joshi<sup>o</sup>, A. Jungclaus<sup>p</sup>,  
K.P. Lieb<sup>q</sup>, A.O. Macchiavelli<sup>r</sup>, F. Moore<sup>i</sup>, G. Mukherjee<sup>i</sup>, A.A. Phillips<sup>a</sup>,  
C. Plettner<sup>k</sup>, W. Reviol<sup>s</sup>, D. Sarantites<sup>s</sup>, H. Schnare<sup>k</sup>, M.A. Schumaker<sup>a</sup>,  
R. Schwengner<sup>k</sup>, D. Seweryniak<sup>i</sup>, M.B. Smith<sup>m</sup>, I. Stefanescu<sup>c</sup>, O. Thelen<sup>c</sup>  
and R. Wadsworth<sup>o</sup>

<sup>a</sup>Department of Physics, University of Guelph, Guelph, Ontario N1G 2W1, Canada

<sup>b</sup>Istituto Nazionale di Fisica Nucleare, Laboratori Nazionali di Legnaro, Legnaro, Italy

<sup>c</sup>Institut für Kernphysik, Universität zu Köln, Zùlpicher Strasse 77, D-50937 Köln, Germany

<sup>d</sup>Department of Physics, University of Notre Dame, Notre Dame, Indiana 46556

<sup>e</sup>Department of Physics and Astronomy, Mississippi State University, Mississippi 39762

<sup>f</sup>Lund Institute of Technology, P.O. Box 118, S-221 00 Lund, Sweden

<sup>g</sup>Oliver Lodge Laboratory, University of Liverpool, Liverpool L69 3BX, UK

<sup>h</sup>McMaster University, Hamilton, Ontario L8S 4K1, Canada

<sup>i</sup>Physics Division, Argonne National Laboratory, Argonne, Illinois 60439

<sup>j</sup>North Carolina State University, Raleigh, North Carolina 27695

<sup>k</sup>Institut für Kern- und Hadronenphysik, FZ Rossendorf, D-01314 Dresden, Germany

<sup>l</sup>Dipartimento di Fisica, Università di Padova and INFN Sezione di Padova, Padova, Italy

<sup>m</sup>TRIUMF, 4004 Wesbrook Mall, Vancouver, British Columbia, V6T 2A3, Canada

<sup>n</sup>CEA Saclay, DAPNIA/SPhN, 91191 Gif-sur-Yvette Cedex, France

<sup>o</sup>Department of Physics, University of York, Heslington, York YO10 5DD, UK

<sup>p</sup>Departamento de Física Teórica, Universidad Autónoma de Madrid, E-28049 Madrid, Spain

<sup>q</sup>II. Physikalisches Institut, Universität Göttingen, D-37073 Göttingen, Germany

<sup>r</sup>Lawrence Berkeley National Laboratory, Berkeley, California 94720

<sup>s</sup>Department of Chemistry, Washington University, St. Louis MO 63130

**Abstract.** High-spin states in  $^{74}_{36}\text{Kr}_{38}$  were studied using the  $^{40}\text{Ca}(^{40}\text{Ca},\alpha 2p)^{74}\text{Kr}$  fusion evaporation reaction at a beam energy of 165 MeV with GAMMASPHERE and MICROBALL and at a beam energy of 185 MeV with EUROBALL and ISIS multi-detector arrays. Lifetimes of the high-spin states for the ground-state band and the favoured negative-parity band have been determined using the Doppler-shift attenuation method. The deduced transition quadrupole moments show a marginal decrease as a function of spin, suggesting that the rotational bands do not terminate at the maximum spin  $I_{max}$ .

**Keywords:**  $^{74}\text{Kr}$ , high spins, lifetimes

**PACS:** 27.50.+e, 21.10.Re, 21.60.Ev, 21.10.Tg

## INTRODUCTION

The understanding of the collective behaviour of nuclei in terms of the microscopic basis of the many-body system is a fundamental goal in nuclear structure. A possibility

to study collective and single particle effects within one nuclear system is given by the band termination phenomenon, which represents a transition from collective to single-particle behaviour. Considerable effort has been devoted to studying band termination in different mass regions, both experimentally and theoretically [1, 2]. Nevertheless it has been predicted theoretically [2, 3, 4] that not all the bands have to terminate in a non-collective state at  $I_{max}$  (maximum spin which can be built in a pure configuration). Recently, the first experimental case has been observed in  $^{74}\text{Kr}$  where the measurements of transitional quadrupole moments  $Q_t$  and mean field calculations strongly suggest that the rotational bands show collectivity at  $I_{max}$  [5].

This manuscript reports on the high-spin states of  $^{74}\text{Kr}$  and their lifetimes. We discuss in detail the measurement of the  $Q_t$  values for high spin states, since these values are decisive in the discussion of the observation of non-termination of the smooth rotational bands in  $^{74}\text{Kr}$  [5].

## EXPERIMENT

High-spin states in  $^{74}\text{Kr}$  were studied using the  $^{40}\text{Ca}(^{40}\text{Ca},2p\alpha)^{74}\text{Kr}$  fusion–evaporation reaction at two different setups. The first experiment was performed at Laboratori Nazionale di Legnaro (LNL), using a 185 MeV beam delivered by the XTU Tandem accelerator. An enriched  $^{40}\text{Ca}$  target was used, with a thickness of  $900\ \mu\text{g}/\text{cm}^2$ . The  $\gamma$  rays produced in the reaction were measured with the EUROBALL III array [6], which was coupled to the  $4\pi$  charged particle detector ISIS [7], and a Neutron Wall [8], which covered the forward  $1\pi$  section of EUROBALL III. The second experiment was carried out at Argonne (ANL), using a 165 MeV beam delivered by the Tandem Linac Accelerator System (ATLAS). The  $\gamma$  rays of the reaction were detected with 99 Compton-suppressed HPGe detectors of the GAMMASPHERE array [9], with the heavymet collimators removed to obtain summed  $\gamma$ -ray energy per event. The evaporated charged particles were detected in coincidence with the  $\gamma$  rays and identified with the 95-element CsI(Tl) MICROBALL detector [10]. A detailed description of both setups can be found in Refs. [5, 11]

## RESULTS AND DISCUSSION

Figure 1 (bottom inset) shows  $\gamma$ -ray coincidence spectra for the ground-state band and the two favoured negative-parity signature partners bands, Band **A** and Band **B**, in  $^{74}\text{Kr}$  deduced from the current analysis. Figure 1 (right) shows the partial decay scheme for  $^{74}\text{Kr}$  deduced from the current work via  $\gamma$ - $\gamma$ - $\gamma$  coincidences. The DCO ratios (see Table 1) have firmly established the spins and parities of the high-spin states. The lack of statistics for the very top transitions did not allow to extract their multipolarity.

Lifetimes of the higher-lying states were measured using the Doppler-shift attenuation method [12] for the ground-state band, Band **A** and Band **B** in  $^{74}\text{Kr}$ . The centroid shifts for a given transition in each of the 16 rings in GAMMASPHERE were measured and the ratio  $F(\tau) = \beta_t/\beta_0$  was plotted versus  $\gamma$ -ray energy. The  $\beta_0$  value is defined by the initial velocity when the recoil was created and was calculated according to the

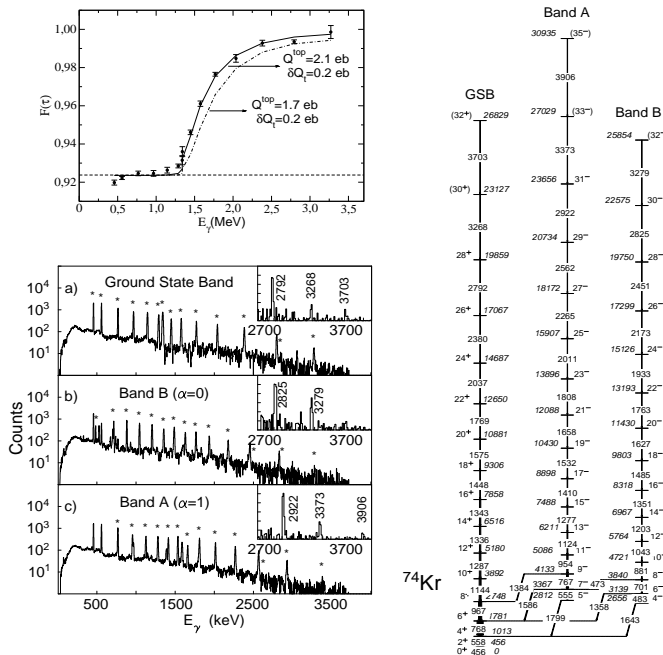


**FIGURE 1.** Partial level scheme deduced from the current work for  $^{74}\text{Kr}$  (right). The bottom inset shows the sum of  $\gamma$ -ray spectra obtained by adding double coincidence gated spectra on in-band transitions in a) the ground-state band of  $^{74}\text{Kr}$ , b) the Band B ( $\alpha = 0$  signature), and c) the Band A ( $\alpha = 1$  signature). In each case, the in-band transitions are denoted by \*. The insets show the highest energy transitions in the mentioned bands as seen in the EUROBALL experiment. The top inset shows the experimental  $F(\tau)$  values for the ground-state band as a function of  $\gamma$ -ray energy in  $^{74}\text{Kr}$ . The solid line shows the fit for a  $Q_t^{top} = 2.1 \text{ eb}$  (best fit), while the dot-dashed line shows the fit considering a lower  $Q_t^{top} = 1.7 \text{ eb}$ . The dashed line represents the saturation  $F(\tau)$  value, when the recoils leave the target.

kinematics of the reaction. The experimental  $F(\tau)$  values were fit taking into account the slowing down process of the recoil in the target, since the  $\gamma$  rays were emitted while the recoils were decelerating in the thin  $^{40}\text{Ca}$  target. The stopping powers were obtained using the SRIM-2003 code [13]. The fitting program takes into account the momentum distribution of the recoils, due to particle emission. It has been shown previously [14, 15] that in the channels where  $\alpha$  particles are present the angular dependence in the particle detection efficiency of MICROBALL is not isotropic and must be included in the lifetime analysis. Figure 1 (top inset) shows the measured  $F(\tau)$  values as a function of  $\gamma$ -ray energy for the ground-state band. The  $F(\tau)$  values were measured by gating on the top three transitions of the band of interest. Side feeding is only considered into those top three states and was modelled assuming a rotational band sequence, with four transitions. The side-feeding quadrupole moment was selected to be the same as in the considered band. The fit of the experimental data was modelled empirically according to

**TABLE 1.** Spin, parities, energies, transition quadrupole moments  $Q_t$  and DCO ratios for the ground-state band (GSB), Band **A** and Band **B** in  $^{74}\text{Kr}$ .

Band GSB						
$iI_n^\pi$	$E_{lvl}(\text{keV})$	$E_\gamma(\text{keV})$	$R_{\text{DCO}}$	$\pm$	$Q_t$ (eb)	$fI_n^\pi$
$(32_1^+)$	26829	3703	–	–	–	$(30_1^+)$
$(30_1^+)$	23127	3268	–	–	$2.10 \pm 0.10$	$28_1^+$
$28_1^+$	19859	2792	0.90	0.17	$2.30 \pm 0.10$	$26_1^+$
$26_1^+$	17067	2380	0.91	0.14	$2.38 \pm 0.10$	$24_1^+$
$24_1^+$	14687	2037	1.01	0.09	$2.45 \pm 0.10$	$22_1^+$
$22_1^+$	12650	1769	0.95	0.08	$2.50 \pm 0.10$	$20_1^+$
$20_1^+$	10881	1575	1.22	0.08	$2.55 \pm 0.10$	$18_1^+$
$18_1^+$	9306	1448	1.00	0.05	$2.59 \pm 0.10$	$16_1^+$
$16_1^+$	7858	1343	1.05	$0.03^*$	$2.63 \pm 0.10$	$14_1^+$
$14_1^+$	6516	1336	1.05	$0.03^a$	$2.67 \pm 0.10$	$12_1^+$
Band A ( $\alpha = 1$ )						
$(35_1^-)$	30935	3906	–	–	–	$(33_1^-)$
$(33_1^-)$	27029	3373	–	–	$2.40 \pm 0.10$	$31_1^-$
$31_1^-$	23656	2922	0.77	0.14	$2.70 \pm 0.10$	$29_1^-$
$29_1^-$	20734	2562	0.91	0.11	$2.82 \pm 0.10$	$27_1^-$
$27_1^-$	18172	2265	1.02	0.08	$2.92 \pm 0.10$	$25_1^-$
$25_1^-$	15907	2011	0.96	0.06	$3.00 \pm 0.10$	$23_1^-$
$23_1^-$	13896	1808	1.14	$0.07^\dagger$	$3.07 \pm 0.10$	$21_1^-$
$21_1^-$	12088	1658	1.01	0.05	$3.14 \pm 0.10$	$19_1^-$
$19_1^-$	10430	1532	1.04	0.05	$3.19 \pm 0.10$	$17_1^-$
$17_1^-$	8898	1410	1.06	0.04	$3.25 \pm 0.10$	$15_1^-$
$15_1^-$	7488	1277	0.99	0.04	$3.30 \pm 0.10$	$13_1^-$
$13_1^-$	6211	1124	gate	–	$3.35 \pm 0.10$	$11_1^-$
Band B ( $\alpha = 0$ )						
$(32_1^-)$	25854	3279	–	–	$2.30 \pm 0.10$	$30_1^-$
$30_1^-$	22575	2825	1.03	0.18	$2.50 \pm 0.10$	$28_1^-$
$28_1^-$	19750	2451	1.14	0.12	$2.58 \pm 0.10$	$26_1^-$
$26_1^-$	17299	2173	1.20	0.11	$2.65 \pm 0.10$	$24_1^-$
$24_1^-$	15126	1933	1.03	0.08	$2.70 \pm 0.10$	$22_1^-$
$22_1^-$	13193	1763	1.05	0.07	$2.75 \pm 0.10$	$20_1^-$
$20_1^-$	11430	1627	1.01	0.05	$2.79 \pm 0.10$	$18_1^-$
$18_1^-$	9803	1485	0.95	0.04	$2.83 \pm 0.10$	$16_1^-$
$16_1^-$	8318	1351	1.14	0.05	$2.87 \pm 0.10$	$14_1^-$

\* doublet

$^\dagger$  doublet with the 1799-keV transition

$Q_t(I) = Q_t^{top} + \delta Q_t \sqrt{I^{top} - I}$  [11]. The *top* superscript indicates the highest-spin state observed experimentally in a given band for the current work, for which a centroid shift could be measured. In the current data, this corresponds to  $I^{top} = 30^+$ ,  $33^-$  and  $32^-$  for the ground-state band, Band **A** and Band **B**, respectively. The  $\delta Q_t$  represents the variation of the  $Q_t$  value within the band. In Fig. 1 (top inset), the solid line represents the best fit to the experimental points ( $Q_t^{top} = 2.1$  eb,  $\delta Q_t = 0.2$  eb), while the dot-dashed line shows the calculated curve considering a smaller  $Q_t^{top}$  ( $Q_t^{top} = 1.7$  eb,  $\delta Q_t = 0.2$  eb).

It can be noted that if a lower  $Q_t^{top}$  is used, then the fit curve will necessarily lie below the experimental points all along the band. Table 1 summarizes the  $Q_t$  values of the measured high-spin states in  $^{74}\text{Kr}$ .

The conclusion about non-termination of three smooth rotational bands in  $^{74}\text{Kr}$  [5], that have been observed up to (or one transition short of) the maximum spin  $I_{max}$ , is based both on the results of mean field calculations [5], and the present measurement of  $Q_t$  values. These rotational bands show marginal decrease of  $Q_t$  with increasing spin. This decrease is much smaller [5] in comparison with other smooth terminating bands, like  $^{62}\text{Zn}$  [16] and  $^{109}\text{Sb}$  [17, 18]. The  $Q_t^{top}$  value obtained in the fitting procedure of  $F(\tau)$  is the smallest one which provides agreement with the experimental curve. Any attempt to make it smaller (i.e. going towards non-collectivity,  $Q_t^{top} \sim 0$ ) moves down the fit  $F(\tau)$  curve relative to the experimental points, increasing the discrepancy with experiment, see Fig. 1 (top inset). A detailed theoretical description of the non-termination of rotational bands in  $^{74}\text{Kr}$  can be found in Ref. [5].

## ACKNOWLEDGMENTS

This work has been partially supported by the NSERC of Canada, the BMBF of Germany under contract number 06K167, the U.K. Engineering and Physical Sciences Research Council, the Swedish Science Research Council, and the U.S. Department of Energy under Contract Nos. DE-AC03-76SF00098, DE-FG02-88ER-40406, DE-F05-96ER-40983 and DE-FG03-03NA0076. C.A. acknowledges the support offered by the Swedish Foundation for Higher Education and Research.

## REFERENCES

1. Ragnarsson, I., Xing, Z., Bengtsson, T., and Riley, M., *Phys. Scripta*, **34**, 1 (1986).
2. Afanasjev, A. V., Fossan, D. B., Lane, G. J., and Ragnarsson, I., *Phys. Rep.*, **322**, 1 (1999).
3. Troudet, T., and Arvieu, R., *Annals of Physics*, **134**, 1 (1981).
4. Ragnarsson, I., and Afanasjev, A. V., *Proc. Conf. on Nuclear Structure at the Limits, Argonne, USA, ANL/PHY-97/1*, 184 (1997).
5. Valiente-Dobón, J. J., et al. (2005).
6. Gerl, J., and Lieder, R. M., Euroball iii, a european  $\gamma$ -ray facility (1992).
7. Farnea, E., et al., *Nucl. Instrum. Methods Phys. Res. A*, **400**, 87 (1997).
8. Skeppstedt, Ö., et al., *Nucl. Instrum. Methods Phys. Res. A*, **421**, 531 (1999).
9. Lee, I. Y., *Nucl. Phys.*, **A520**, 641c (1990).
10. Sarantites, D. G., et al., *Nucl. Instrum. Methods Phys. Res. A*, **381**, 418 (1996).
11. Valiente-Dobón, J. J., et al., *Phys. Rev. C*, **71**, 034311 (2005).
12. Cederwall, B., *Nucl. Instrum. Methods Phys. Res. A*, **354**, 591 (1995).
13. Ziegler, J. F. (2003).
14. Svensson, C. E., et al., *Acta Phys. Pol.*, **B9**, 2413 (2001).
15. Chiara, C. J., et al., *Nucl. Instrum. Methods Phys. Res. A*, **523**, 374 (2004).
16. Svensson, C. E., et al., *Phys. Rev. Lett.*, **80**, 2558 (1998).
17. Wadsworth, R., et al., *Phys. Rev. Lett.*, **80**, 1174 (1998).
18. Vretenar, D., Afanasjev, A. V., Lalazissis, G. A., and Ring, P., *Phys. Rep.*, **409**, 101 (2005).